Bessel functions and distort the contours of integration into the first and fourth quadrant of the complex λ-plane. Integrals involving $H_0^{(2)}(\lambda\rho)$ are evaluated in the fourth quadrant and those with $H_0^{(1)}(\lambda\rho)$ in the first quadrant. The integrals are then completely specified by the residues in the first and fourth quadrant.

However, we may simplify the evaluation by imposing the argument that there can be no poles in the fourth quadrant as such poles would generate space waves which would not satisfy the radiation condition as $\rho \to \infty$.[4] The integrals are then evaluated as

$$I_1(\rho) = 2\pi i \sum \text{Residues} \cdot \left[\frac{2\pi(\lambda^2 - k_a^2)\lambda H_0^{(1)}(\lambda\rho)}{2\Delta(\lambda)}\right]_{1st}, \quad (11)$$

$$I_2(\rho) = 2\pi i \sum \text{Residues} \cdot \left[\frac{2\pi\lambda^3 H_0^{(1)}(\lambda\rho)}{2\Delta(\lambda)}\right]_{4th} \quad (12)$$

The poles of the integrands in I_1 and I_2 are determined by the roots of $P(\lambda)$ given above. We find for the magnetic field and pressure the following expressions:

$$H_y(\rho) = \frac{\omega\epsilon_0\epsilon J_0}{4\epsilon_1(1-\beta)}\left\{\frac{(k_{mp}^2 - k_a^2)}{(k_{mp}^2 - k_{m0}^2)} H_0^{(1)}(k_{mp}\rho) + \frac{(k_{m0}^2 - k_a^2)}{(k_{m0}^2 - k_{mp}^2)} H_0^{(1)}(k_{mp}\rho)\right\}, \quad (13)$$

$$P(\rho) = \frac{B_0 X J_0}{4(1-X)} \frac{\omega\epsilon_0\epsilon}{\epsilon_1(1-\beta)} \cdot \left\{\frac{k_{mp}^2}{k_{mp}^2 - k_{m0}^2} H_0^{(1)}(k_{mp}\rho) + \frac{k_{m0}^2}{k_{m0}^2 - k_{mp}^2} H_0^{(1)}(k_{m0}\rho)\right\}. \quad (14)$$

The optical and plasma modes are described by the wave numbers k_{m0} and k_{mp} respectively. Assuming the velocity of sound is much less than the velocity of light ($a \ll c$) in the electron plasma, the wave numbers may be expressed as

$$k_{m0}^2 \doteq B(1 - \sqrt{1 - C/B^2}),$$

$$k_{mp}^2 \doteq B(1 + \sqrt{1 - C/B^2}). \quad (15)$$

where

$$2B = (\omega^2/a^2 + \omega^2/c^2)(1 - X - Y^2),$$

$$C = \frac{\omega}{a^2c^2}[(1-X)^2 - Y^2].$$

To discuss the propagation characteristics, we need only consider the range of values for the parameters X and Y. For this purpose we define the "parameter plane" defined with X and Y as coordinates. In this plane the critical curves are those for which $B=0$ and $C=0$. These curves are plotted in Fig. 1.

From this plot it is now a simple matter to determine the regions of the $X=Y$ plane

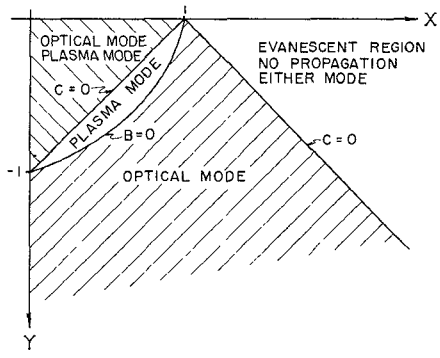

Fig. 1—Optical-plasma radiation characteristics.

in which the optical mode or the plasma mode are propagating or evanescent. Indeed one finds the modes propagate as illustrated in Fig. 1. The optical mode exhibits "cutoff" characteristics along the lines defined by $(1-X)^2 - Y^2 = 0$ and $1 - X - Y^2 = 0$. The plasma mode has only cutoff characteristics defined by $1 - X - Y^2 = 0$. It is now quite clear as to what values of parameters, X and Y, are critical in the excitation of radiation modes in a compressible plasma. Power splitting between the modes is now a relatively simple matter for the regions indicated in Fig. 1.

K. R. Cook
Dept. of Elec. Engrg.
Oklahoma State University
Stillwater, Okla.

Quasi-Optical Waveguide Filters

Oversize rectangular waveguide operating in the TE_{10} mode is useful in constructing components operating at millimeter and submillimeter wavelengths [1], [2]. This communication describes preliminary results on quasi-optical oversize waveguide filters. It is easier to construct filters using this technique and they have lower attenuation loss than conventional-size waveguide filters. When the waveguide is appreciably oversize (10 or more times standard-size TE_{10} waveguide), a good approximation to plane wave propagation exists. This enables gratings and dielectric slabs to be used in a way that is similar to their application in optical structures, which have previously been considered as filter-like elements at millimeter and submillimeter wavelengths [3], [4], [5]. We have examined the problems of making multi-element filters in oversize waveguide using the techniques of free-space optics modified appropriately for the oversize waveguide. We will describe in detail a two-port metallic grating and a four-port dielectric-slab filter.

A typical two-port band-pass metallic-grating structure can be constructed in oversize waveguide using quasi-optical techniques. The filter consists of n resonators, each resonator being q half wavelengths long. A typical grating consists of many regularly spaced iris holes in a flat metallic plate. Any coupling coefficient value can be obtained by choosing holes of the proper diameter.

The design theory for this filter, for the calculation of coupling susceptance, is similar to that for waveguide filters using standard-size waveguide except that standard coupling structures such as irises and slits cannot be used. To prevent higher modes from being produced, it is necessary to operate uniformly on the plane-wave front. Uniform operation is possible if the coupling is distributed throughout the surface that connects the two resonators. We have constructed and evaluated a filter of this type at 9 mm in a design that can be scaled to the submillimeter region.

This experimental two-resonator band-pass filter was designed in S-band waveguide. It operated at 32.775 Gc with a 22.5 Mc bandwidth and a 1.7 db insertion loss at its center frequency. Each resonator was five half-wavelengths long. A similar design in conventional waveguide (WR28 coin-silver waveguide) using a Q_u 60 per cent of theoretical, would have had a 6.6 db insertion loss. Fig. 1 shows the completed filter. The outer coupling holes are 0.104 inch in diameter and the inner holes are 0.053 inch in diameter. Each plate has 105 holes.

A graph of the insertion loss versus frequency for the oversize waveguide filter is shown in Fig 2. This figure also shows the insertion loss vs frequency characteristics at frequencies where each cavity was six half-wavelengths long. A scaled version is now under construction for operation at 330 Gc. In addition, we are studying quarter-wavelength dielectric-slab filters with similar characteristics.

A typical four-port dielectric-slab filter consists of a pair of parallel dielectric slabs, oriented at 45° in relation to the incident radiation, of thickness t, and separated by an air space d. This device couples power from port 1 to ports 2 and 4; no power is coupled to port 3, and port 1 is matched (Fig. 3).

The power transmitted from port 1 to port 2 is a function of d and λ. The multiple-slab structure can be used as a variable attenuator or as a directional coupler in addition to being used as a low-pass/high-pass filter. The preliminary evaluation and analysis of this filter has emphasized coupling properties (at a fixed frequency) with respect to the variation in d. The actual device was tested at 0.9 mm with a CSF carcinotron; it was far more practical to vary the slab separation than to vary the incident wavelength. The carcinotron was not operable over a wide enough bandwidth for meaningful testing nor could its frequency be determined very accurately. A theoretical analysis of the expected perfornance of the device was made for the single-frequency condition [1]. This analysis is readily modi-

[4] B. B. Baker and E. T. Copson, "The Mathematical Theory of Huygens' Principle," Oxford University Press, London, England; 1950.

Manuscript received June 1, 1964, revised July 21, 1964. The work reported here is based on a paper delivered at the 1964 PTGMTT Symposium, New York, N. Y. This work was supported in part by Rome Air Development Center, Griffiss Air Force Base, N. Y., under Contract AF 30(602)-2758.

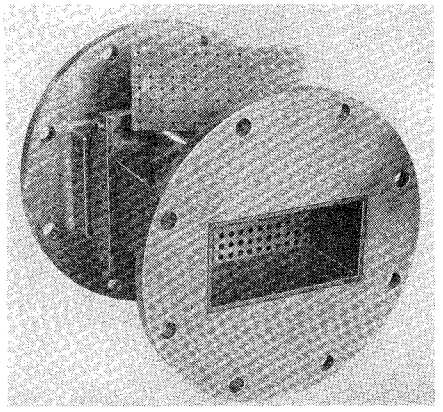

Fig. 1—Two-resonator quasi-optical filter.

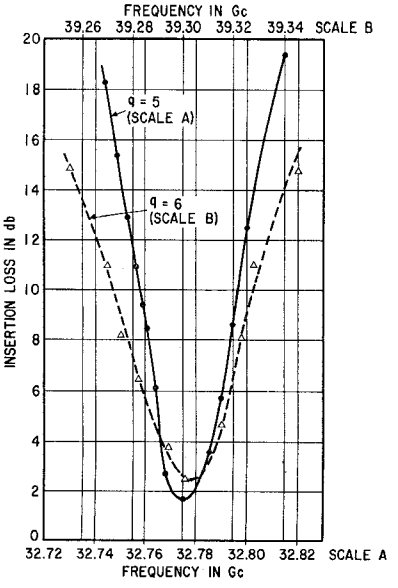

Fig. 2—Insertion loss vs frequency of quasi-optical two-resonator filter.

fied for the case of constant separation and varying frequency. At present, we have inferred proper filter action from the single-frequency data that will be described in the following paragraphs.

Taub, *et al.* [1] gives curves that describe the single-frequency operation for one and two pairs of slabs for materials with various dielectric constants. These curves indicate that the transmitted power rises and falls with a periodicity of 127 electrical degrees; this is approximately a 12-db attenuation range for a single pair of quartz slabs. Thus, such a structure is limited to low coupling ratios—that is, it is limited in its maximum insertion loss when used as a filter. To obtain a greater range of insertion loss, the multiple-slab structure using two pairs of slabs was used. This device has a theoretical range of 27 db.

An analysis of the dissipation loss in this multiple-slab filter has been made and appears in Taub and Hindin [6]. The purpose of the analysis was to estimate the dielectric losses of the device. The analysis is valid for any number of slabs. Since quartz slabs are used, we can estimate the loss by using measured values of ϵ_r and tan δ. At 0.9 mm, $\epsilon_r = 3.9$ and tan $\delta = 0.0043$ [7]. Using [6] we

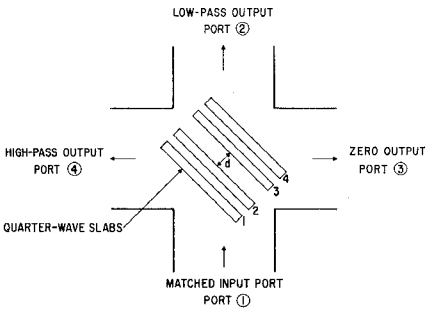

Fig. 3—High-pass and low-pass directional filter.

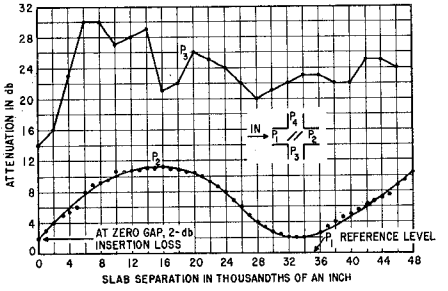

Fig. 4—$n = 2$ multiple-slab test data.

obtain a theoretical insertion loss of 0.65 db. The filter was tested at 0.9 mm using a CSF COE 10 carcinotron. Fig. 4 shows the data obtained.

This is in reasonable agreement with the theoretical characteristics shown in Taub and Hindin [6]. There was sufficient range in the slab separation to permit the periodicity and the filter response attenuation characteristics to be shown. The device had only 2 db of insertion loss. This value is higher than predicted and it is felt that the discrepancy is mainly due to nonperfect alignment of the slabs, which causes a leakage of power into the perpendicular arm. This accounts for about 1 db. Wall losses, loss in the quartz slabs, and the imperfect directivity (matching) of the device account for 0.2 to 0.3 db more.

The separation between peaks of the filter characteristic should be 127° and is measured to be 126°. This again verifies the quasi-optical design theory. The only failure in this device is its inability to obtain the theoretical maximum attenuation for a given slab separation. We believe this discrepancy is related to the apparent higher insertion loss. The directivity of the filter is also shown in Fig. 4. It varies between 10 and 20 db, but will probably be improved when the cause of the decreased attenuation range is determined.

The data presented indicate the feasibility of the techniques for constructing quasi-optical filters. Work is continuing on these devices and will be reported in a future publication.

J. J. Taub
H. J. Hindin
G. P. Kurpis
Applied Electronics Dept.
Airborne Instruments Lab.
A Division of Cutler-Hammer, Inc.
Deer Park, Long Island, N. Y.

References

[1] J. J. Taub, H. J. Hindin, O. F. Hinckelmann, and M. L. Wright, "Submillimeter components using oversize quasioptical waveguide," IEEE Trans. on Microwave Theory and Techniques, vol. MTT-11, pp. 338–345; September, 1963.
[2] J. J. Taub and H. J. Hindin, "Design of quasioptical components," *Microwave*, vol. 3, pp. 20–29; January, 1964.
[3] W. Culshaw, "Reflectors for a microwave Fabry-Perot interferometer," IRE Trans. on Microwave Theory and Techniques, vol. MTT-7, pp. 221–228; April, 1959.
[4] L. Young and P. W. Baumeister, "Microwave and Optical Interference Filters—Some Similarities and Differences," *NEREM Record*, pp. 8–9; 1963.
[5] R. Ulrich, K. F. Renk, and L. Genzel, "Tunable submillimeter interferometers of the Fabry-Perot type," IEEE Trans. on Microwave Theory and Techniques, vol. MIT-11, pp. 363–369; September, 1963.
[6] J. J. Taub and H. J. Hindin, "Final Report on Submillimeter Wave Component Development," TDR-RADC-63-237; May, 1963.
[7] J. J. Taub and H. J. Hindin, "Permittivity measurements at submillimeter wavelengths," *Rev. Sci. Instr.*, vol. 34, pp. 1056–1057; September, 1963.

Total System Noise Temperature: 15°K

Laboratory evaluation of an operational maser system has led to interesting results, particularly in regard to accurate noise temperature measurements.

The maser is a ruby loaded comb structure designed for operation at 2295 Mc. It is normally operated with 37 db gain and 18 Mc of 3-db bandwidth, at a refrigerator temperature of 4.5°K. The maser is conduction cooled for hard-vacuum operation in a closed-cycle helium refrigerator.[1]

The package containing the maser and refrigerator weighs 450 pounds. A 180-pound magnet supplies a 2500 gauss field. The package also contains a klystron pump oscillator, a noise calibration package, directional couplers for gain and noise temperature measurements, heaters, and a thermistor to maintain constant package temperature (see Fig. 1).

Several components affect the equivalent input temperature of the maser. A 26-db crossguide coupler and a transition to a $\frac{7}{8}$ coaxial line precede the maser. A $\frac{7}{8}$ inch 50 ohm coaxial feeds the input signal through the vacuum jacket into the maser. Careful construction techniques have resulted in a combination of low insertion loss and good thermal isolation.

In order to accurately measure the equivalent input temperature of the maser, a standard neon noise source is used in conjunction with terminations at liquid helium, liquid nitrogen, and ambient temperatures. The liquid-helium-cooled termination has been constructed in WR 430 *S*-band waveguide. The thin wall (0.025 inch) stainless steel waveguide gives adequate thermal isolation and results in a useful operating life of

Manuscript received July 30, 1964. This paper represents one phase of research carried out at the Jet Propulsion Lab., Pasadena, Calif., under contract No. NAS 7-100; sponsored by NASA, Washington, D. C.

[1] The traveling wave maser was purchased from Airborne Instruments Laboratory. The "Cryodyne" helium refrigerator was purchased from Arthur D. Little, Inc., Cambridge, Mass.